

Supporting information

Molecular Coupling between Organic Molecules and Metal

Pengcheng Hu, Xu Li, Bolin Li, Xiaofeng Han, Furong Zhang, Keng C. Chou, Zhan Chen, and Xiaolin Lu

As demonstrated in the main text, to prepare a compact SAM layer on the substrate, the immersion times for all the SAM samples were controlled to be ~12 h. We recorded the curve of the contact angle versus the immersion time for each SAM sample, as shown in Figure S1. By transferring the time-dependent contact angle into the apparent surface coverage^{S1}, the apparent surface coverages for all the SAMs were calculated, all of which are more than ~99%.

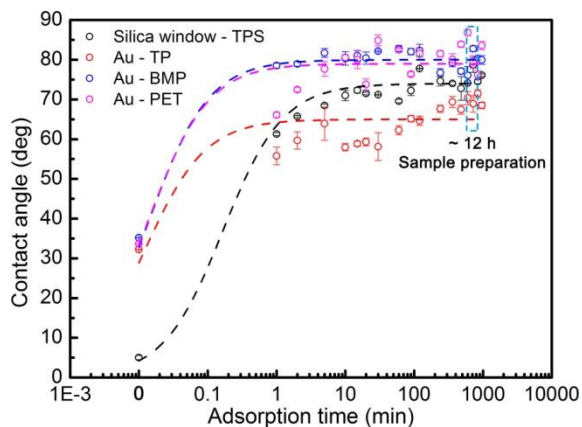


Figure S1. Water contact angles versus the immersion time for SAMs of TP, BMP, PET on Au, and SAM of TPS on silica respectively. The lines are used as a guide.

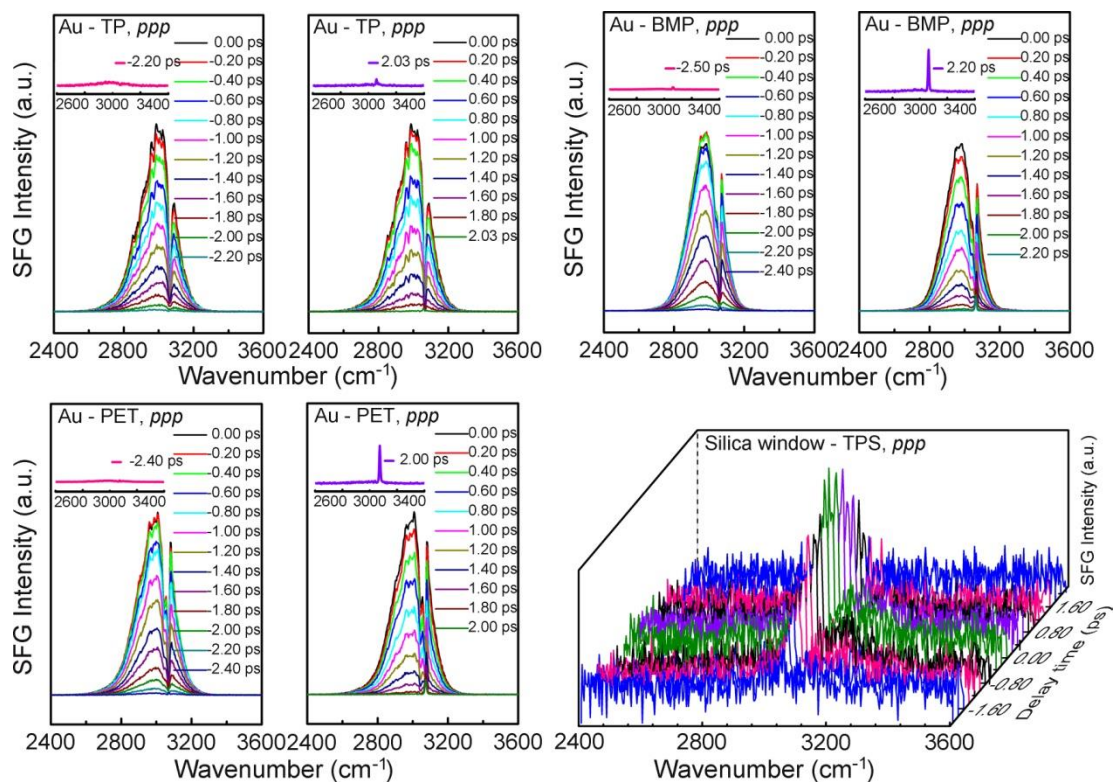


Figure S2. The frequency-domain spectra for SAMs of TP, BMP, PET on Au, and SAM of TPS on silica in the C-H stretching region as a function of the delay time.

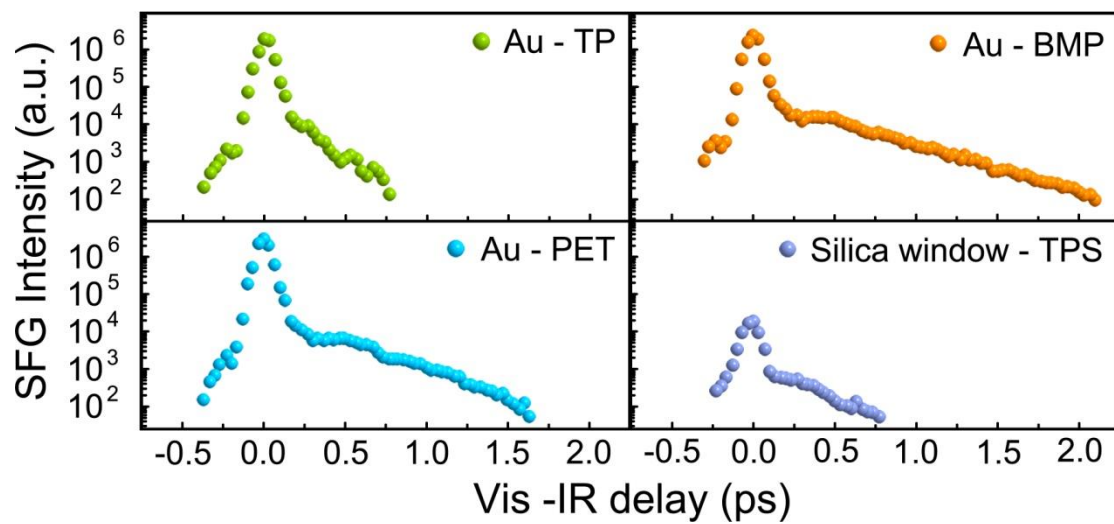


Figure S3. The original FID data for SAMs of TP, BMP, PET on Au, and SAM of TPS on silica.

Fitting

In order to fit the SFG FID, first the frequency domain SFG spectra need to be fitted using the following equation ^{S2,S3}:

$$I_{SFG} \propto \left| \sum_n \frac{A_n}{\omega_{IR} - \omega_n + i(\Gamma_n + \Delta\omega_{vis}/2)} e^{i\varepsilon_n} + \frac{|A_{NR}|}{\Delta\omega_{IR}} \right|^2 \times \exp\left\{-\left(\frac{\omega_{IR} - \omega_0}{\Delta\omega_{IR}}\right)^2\right\} \quad (S1)$$

where A_n , ε_n , and Γ_n represent the amplitude of the surface vibration with frequency ω_n , the phase between the resonant and nonresonant contributions, and the damping constant, respectively. A_{NR} is the nonresonant contribution. ω_0 represents the center frequency of the incident IR pulse. $\Delta\omega_{IR}$ and $\Delta\omega_{vis}$ represent the spectral width of the IR and visible pulse, respectively.

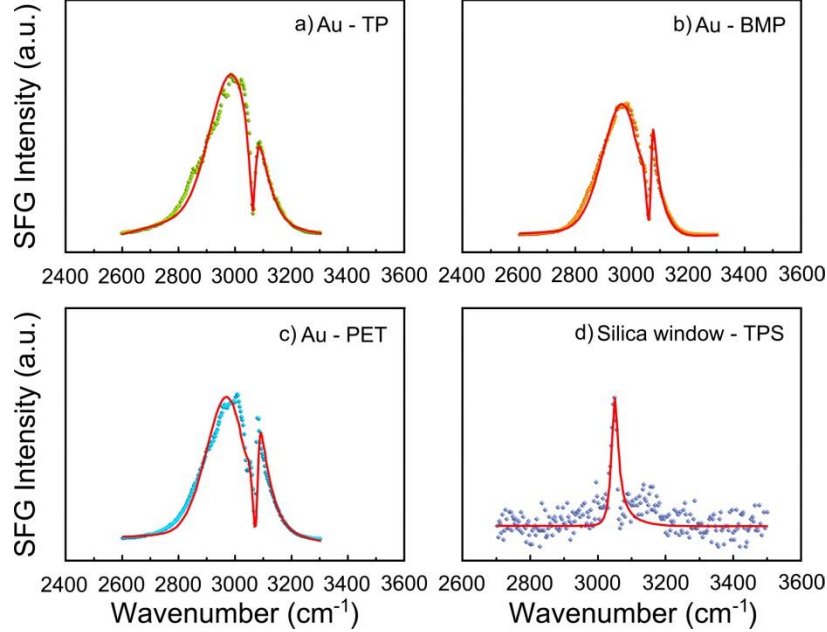


Figure S4. The frequency-domain SFG spectra and the fitted results using Equation S1.

Based on the previous theoretical and experimental work of Mii, Ueba, Borguet, Benderskii and Bonn groups^{S3-S7}, when the delay time between IR and visible pulses is t_d , the SFG intensity can be expressed as

$$I_{SFG-FID}(t_d) \propto \int_{-\infty}^{\infty} dt |P^{(2)}(t, t_d)|^2 \quad (S2)$$

$$P^{(2)}(t, t_d) \propto E_{vis}(t - t_d) P^{(1)}(t) \quad (S3)$$

In above equations, the 1st order polarization induced by the IR beam can be expressed as

$$P^{(1)}(t) = \int_{-\infty}^{\infty} dt' E_{IR}(t - t') S(t') \quad (S4)$$

The time responsive function, $S(t')$ in Equation S4, could be obtained from Equation S5, which contains the delta function $\delta(t)$ and the Heaviside step function, where c is the speed of light, and $1/(2\pi c\Gamma_n)$ is the total dephasing time of n th vibrational mode ($T_{2,n}$).

$$S(t) = \left[\delta(t) |A_{NR}| \exp(i\varepsilon) - i\theta(t) \sum_n A_{R,n} \times \exp\{2\pi c(-i\omega_n t - \Gamma_n t)\} \right] + c.c. \quad (S5)$$

Finite pulse widths with a Gaussian profile for the IR and visible beams, as shown in Equations S6 and S7, were used.

$$E_{IR/Vis}(t) = E_{IR/Vis} \exp(-t^2/\tau^2 - i2\pi c\omega_{IR/Vis}t) + c.c. \quad (S6)$$

$$\bar{E}_{IR}(\omega) = \bar{E}_{IR} \exp(-(\omega - \omega_0)^2 / \Delta\omega_0^2) \quad (S7)$$

where $E_{IR/Vis}$ represents the magnitude of $E(t)$ for either IR or visible and τ is its pulsewidth. The 1st order polarization generated by the infrared pulse can thus be written as

$$P^{(1)}(t) = P_{NR}^{(1)}(t) + P_R^{(1)}(t) + c.c. \quad (S8)$$

$$P_{NR}^{(1)}(t) = |A_{NR}| \exp(-t^2/\tau^2 + i\varepsilon - i2\pi c\omega_0 t) \quad (S9)$$

$$P_R^{(1)}(t) = -\int_{-\infty}^t e^{-(t'^2/\tau^2)} dt' \sum_n iA_{R,n} \times \exp\left[-\left\{(\omega_n - \omega_0)^2 / \Delta\omega_{IR}^2\right\}\right] \times \exp\{2\pi c(-i\omega_n t - \Gamma_n t)\} \quad (S10)$$

Table S1. Fitting parameters for the damping process in the time-domain measurement.

Classes	Sample	Dephasing time from segmental fitting and quantum beating fitting (ps)					
		Surface free electrons		Shoulder mode of phenyl		Strong mode of phenyl	
		Segmental fitting	Quantum beating	Segmental fitting	Quantum beating	Segmental fitting	Quantum beating
Apparent three segments	Au – BMP	0.053 ± 0.002	/	0.24 ± 0.02	0.25 ± 0.02	0.66 ± 0.02	0.67 ± 0.04
	Au – PET	0.055 ± 0.002	/	0.20 ± 0.03	0.21 ± 0.01	0.65 ± 0.02	0.61 ± 0.06
		Surface free electrons or nonresonant polarization		Phenyl vibrational mode			
		Segmental fitting	Quantum beating			Segmental fitting	Quantum beating
Apparent two segments	Au – TP	0.058 ± 0.002	/			0.28 ± 0.02	0.28 ± 0.03
	Silica window – TPS	0.067 ± 0.002	/			0.61 ± 0.01	0.60 ± 0.03

References

- S1. Liu, Y.; Wolf, L. K.; Messmer, M. C. *Langmuir* 2001, 17, 4329–4335.
- S2. Du, Q.; Superfine, R.; Freysz, E.; Shen, Y. R. *Phys. Rev. Lett.* **1993**, 70, 2313–2316.
- S3. Nihonyanagi, S.; Eftekhari-Bafrooei, A.; Borguet, E. *J. Chem. Phys.* **2011**, 134, 084701/1–084701/7.
- S4. Bordenyuk, A. N.; Jayathilake, H.; Benderskii, A. V. *J. Phys. Chem. B* **2005**, 109, 15941–15949.
- S5. Mii, T.; Ueba, H.; *Surf. Sci.* **1999**, 427–428, 324–330.
- S6. Ueba, H.; Sawabu, T.; Mii, T. *Surf. Sci.* **2002**, 502–503, 254–260.
- S7. Roke, S.; Kleyn, A. W.; Bonn, M. *Surf. Sci.* **2005**, 593, 79–88.